

3. N. D. Sosnovski, "Hydrodynamics and the process of separating solid particles in rotating channels with contoured boundaries," Author's Abstract of Candidate Dissertation in the Physical-Mathematical Sciences, Leningrad Polytechnic Institute, Leningrad (1988).
4. W. P. Jones and B. E. Launder, "Prediction of laminarization with a two-equation model of turbulence," Intern. J. Heat Mass Transfer., 15, No. 2 (1972).
5. Launder, Pridden, and Sharma, "Calculation of a turbulent boundary layer on rotating curvilinear surfaces," Trans. Am. Soc. Eng. Mechanics. Theoretical Basis for Engineering Calculations, No. 1 (1977).
6. U. Frost and T. Moulden (eds.), Turbulence, Principles and Applications [Russian translation], Mir, Moscow (1980).
7. L. A. Dorfman, Numerical Methods in the Hydrodynamics of Turbines [in Russian], Énergiya, Leningrad (1974).
8. E. Bakke, J. F. Kreider, and F. Kreith, "Turbulent source flow between parallel stationary and co-rotating disks," J. Fluid Mech., 58, Part 2 (1973).

SEDIMENTATION OF A CLOUD OF A BIDISPERSED AEROSOL ONTO A FLAT  
HORIZONTAL SURFACE

G. M. Makhviladze, D. V. Serov, and S. E. Yakush

UDC 532.529

A characteristic feature of the motion of a cloud of monodispersed particles in the open under the influence of gravity is the clear appearance of collective effects, which result from the hydrodynamic interaction of the falling particles through a gaseous carrier. Depending on the degree of this interaction, it is convenient to distinguish two sedimentation regimes [1, 2]. In the entrainment regime, the particles completely or partially entrain the medium between them; as a result, the falling velocity of an aggregate of particles exceeds the velocity of a single particle, and the cloud takes on the shape of a bowl or a torus. In the filtration regime, the particles settle out practically independent of each other, the velocity of the center of mass of the cloud equals the falling velocity of a single particle, and the cloud shape changes extremely slowly. The entrainment regime occurs if there is a large enough concentration of fine particles in the cloud [2]. As the particle dimension increases or their concentration decreases, there is a transition to the filtration regime.

Particles of identical dimensions (monodispersed aerosol) have been examined in theoretical studies [2-5] on the free sedimentation of an aggregate of fine particles under the force of gravity. Actually, real aerosol formations usually consist of particles of various dimensions. The most extensive situation is the one where particles can be separated into two characteristic dimensions (bidispersed aerosol). An example is natural rain clouds, which consist of mist and rain drops.

Here an approach investigate monodispersed aerosols [2] is generalized to the case of a bidispersed cloud. It is shown that as this cloud settles out, it either divides into two independently moving monodispersed clouds or settles as a single one. The conditions are found for which each of these regimes is realized. The dispersion laws of particles on the sedimentation surface are also found.

1. Let a cloud of solid or liquid spherical particles of two types be formed in a quiescent gas above a flat horizontal surface at time  $t = 0$ . The particles are of the same material and differ only in diameter. They start to move downwards due to the force of gravity and leave the suspending gas behind. The problem is to calculate the transient motion of the particles and the gas until all the particles have settled out on the underlying surface. It is assumed that the dimension of the cloud in one of its horizontal directions is much larger than the other, which makes it possible to seek a solution independent of one of

the spatial coordinates - the plane problem. (It has been shown [6], all the laws characteristic for the plane case, are also retained with a high degree of accuracy for an axisymmetric cloud.) The basic assumption of mechanically continuous media [7] - the possibility of describing the system as a combination of three interacting and interpermeating continuous media: gas and particles with diameters  $d_1$  and  $d_2$ . A cloud with a low volume content of the dispersed phase is examined, so that the collisions of the particles with each other can be neglected. The processes of evaporation, adhesion, and breakup are assumed insignificant. The particles interact only through the gas via the interphase transfer of momentum. Heating of the gas due to viscous dissipation is small, and the process can be considered isothermal.

With these assumptions, the two-dimensional transient motion of a heterogeneous mixture is described by the following equations [7], which are written in a dimensionless form: for the carrier gas

$$\frac{d_1 \rho_1}{dt} = -\rho_1 \operatorname{div} \mathbf{V}_1 \left( \frac{d_1}{dt} = \frac{\partial}{\partial t} + u_1 \frac{\partial}{\partial x} + v_1 \frac{\partial}{\partial y} \right); \quad (1.1)$$

$$\rho_1 \frac{d_1 \mathbf{V}_1}{dt} = -\frac{1}{\gamma M^2} \nabla P + \frac{1}{\operatorname{Re}_e} (\Delta \mathbf{V}_1 + \operatorname{grad} \operatorname{div} \mathbf{V}_1) - \mathbf{f}_1 - \mathbf{f}_2 - \rho_1 \mathbf{j}; \quad (1.2)$$

$$P = \rho_1 (\gamma = c_p/c_v \quad M^2 = Rg/(\gamma R_0 T_0), \quad \operatorname{Re}_e = R \sqrt{Rg\rho_{10}/\eta_e}); \quad (1.3)$$

and for two types of particles

$$\frac{d_{2i} \rho_{2i}}{dt} = -\rho_{2i} \operatorname{div} \mathbf{V}_{2i} \left( \frac{d_{2i}}{dt} = \frac{\partial}{\partial t} + u_{2i} \frac{\partial}{\partial x} + v_{2i} \frac{\partial}{\partial y} \right); \quad (1.4)$$

$$\rho_{2i} \frac{d_{2i} \mathbf{V}_{2i}}{dt} = \mathbf{f}_i - \rho_{2i} \mathbf{j} \quad (i = 1, 2). \quad (1.5)$$

Here  $t$  is time;  $x$  and  $y$  are the Cartesian coordinates (the  $x$  axis is directed along the underlying surface), the  $y$  axis is vertically upwards, and the origin of the coordinates is at the surface under the center of mass of the cloud); the index 1 denotes the gas, 2 the particles, and the second index indicates the type of particle;  $\rho$  is the average density;  $\mathbf{V} = (u, v)$  is the velocity;  $P$  is the gas pressure;  $\mathbf{j}$  is the unit vector in the vertical direction;  $\gamma$  is the adiabatic index;  $M$  is the Mach number;  $\operatorname{Re}_e$  is the effective Reynolds number; and  $\eta_e$  is the effective viscosity. The characteristic scales for deriving the dimensionless quantities are the radius of the cloud  $R$ , the velocity  $\sqrt{Rg}$  ( $g$  is the acceleration due to gravity in a vacuum), the time  $\sqrt{R/g}$ , the gas density  $\rho_{10}$  at the surface  $y = 0$ , the pressure  $\rho_{10} R_0 T_0$  ( $R_0$  is the gas constant and  $T_0$  is the temperature of the medium, assumed constant). The concentration of the  $i$ -th type of particle  $n_{i1}$ , which is maximum in the center of the cloud and is  $n_{i0}$  at time  $t = 0$ , and the diameter  $d_i$  of the particles of the  $i$ -th type all determine the volume fraction  $\alpha_{2i}$  of particles of the  $i$ -th type in the cloud; in dimensional quantities

$$\alpha_{2i} = n_{i1} \pi d_i^3 / 6 \quad (\alpha_{2i}^0 = n_{i0} \pi d_i^3 / 6).$$

The volume fraction can be used to interrelate the dimensionless average density of the particles  $\rho_{2i}$  and their concentration (equal to the ratio of the dimensional concentration of the particles to  $n_{i0}$ ):

$$\rho_{2i} = \alpha_{2i}^0 \varepsilon n_i \quad (\varepsilon = \rho_{10} / \rho_2^0)$$

where  $\rho_2^0$  is the actual density of the material in the dispersed phase.

The volume force for interaction between the gas and the particles of the  $i$ -th type is expressed in the form [7]

$$\mathbf{f}_i = \frac{3}{4} \frac{\varepsilon}{\delta_i} C_{di} (\operatorname{Re}_{pi}) \rho_1 \rho_{2i} |\mathbf{V}_1 - \mathbf{V}_{2i}| (\mathbf{V}_1 - \mathbf{V}_{2i}),$$

$$\operatorname{Re}_{pi} = \operatorname{Re}_{pi}^0 \rho_1 |\mathbf{V}_1 - \mathbf{V}_{2i}|, \quad C_{di} = 24 / \operatorname{Re}_{pi} (1 + 0,158 \operatorname{Re}_{pi}^{2/3}), \quad \delta_i = d_i / R,$$

where  $\operatorname{Re}_{pi}^0 = d_i \rho_{10} \sqrt{Rg} / \eta$  is the Reynolds number of particles of type  $i$ ; and  $C_{di}$  is the drag coefficient. In further discussion, it is convenient to introduce a Reynolds number  $\operatorname{Re}^0 =$

$R\sqrt{Rg\rho_{10}}/\eta$ , which is based on the characteristic dimension of the cloud and the molecular viscosity of the gas  $\eta$ ; then  $Re_{pi}^0 = Re^0\delta_i$ .

The boundary conditions consider the symmetry relative to the plane  $x = 0$

$$\begin{aligned} u_1 &= 0, \partial v_1/\partial x = 0, \partial \rho_1/\partial x = 0, \\ u_{2i} &= 0, \partial v_{2i}/\partial x = 0, \partial \rho_{2i}/\partial x = 0 \quad (i = 1, 2), \end{aligned} \quad (1.6)$$

the unperturbed state of the gas at infinity ( $x^2 + y^2 \rightarrow \infty$ )

$$u_1 = v_1 = 0, \partial P/\partial y = -\gamma M^2 \rho_1, \quad (1.7)$$

and the adhesion condition  $u_1 = v_1 = 0$  at the plane  $y = 0$ . Particle collisions with the surface are assumed to be absolutely inelastic - all the particles that reach the surface remain on it.

At time  $t = 0$ , the following distribution of the dimensionless particle concentration

$$n_i(x, y) = \exp [-(x^2 + (y - H)^2)] \quad (i = 1, 2) \quad (1.8)$$

is assigned to a quiescent gas in a state of equilibrium [the conditions (1.7) are fulfilled throughout the whole region]. In Eq. (1.8),  $H = H_0/R$ , where  $H_0$  is the height of the center of the cloud above the surface.

The solution to the problem in dimensionless variables depends on the defining parameters

$$\gamma M^2, Re_e, \alpha_{2i}^0, \varepsilon, \delta_i, Re^0, H \quad (i = 1, 2). \quad (1.9)$$

For clouds with  $R \geq 1$  m, the effective Reynolds number is rather large ( $Re_e \geq 10^5$ ). That is, the gas motion is turbulent, which is considered below in the choice of the corresponding  $Re_e$ , which is constructed from  $\eta_e$ , which is much larger than its value in laminar flow. At the same time, because the particle diameter is much less than the characteristic scale of turbulence,  $Re^0$  is determined by the molecular viscosity. Thus  $Re_e$  and  $Re^0$  can be considered as independent parameters [2].

The system of Eqs. (1.1)-(1.5) with the boundary and initial conditions (1.6)-(1.8) are solved numerically by methods discussed in [8, 9]. The calculations use a constant value  $\gamma M^2 = 10^{-3}$ ,  $\varepsilon = 10^{-3}$ , and  $Re_e = 29$ . The other parameters were chosen in the following ranges:  $\alpha_{21}^0 = 10^{-4} - 2 \cdot 10^{-3}$ ,  $\delta_1 = 2 \cdot 10^{-6} - 8 \cdot 10^{-4}$ ,  $Re^0 = (1-26) \cdot 10^6$ , and  $H = 5-15$ .

2. The calculations showed that, depending on the values of the defining parameters, the bidispersed cloud either moves as a whole (combined sedimentation regime, see paragraph 3) or, due to the weak hydrodynamic interaction between the particles of different diameters, the larger particles, which settle with a higher velocity, settle from the bidispersed cloud independently of the fine ones. In the last case, the initially given bidispersed cloud separates into two independent monodispersed clouds, and the characteristics of the evolution and sedimentation of each of them can be found from the results of [2]. The new problem, which requires additional study, is to determine the conditions for realizing each of the above sedimentation regimes.

The boundary between the regimes in the space of the defining parameters was established by calculating the maximum distance between the centers of mass of the two types of particles over time. This distance is found from the formula

$$y_{ci}(t) = \int_0^\infty \int_0^\infty \rho_{2i}(x, y, t) y dx dy / \int_0^\infty \int_0^\infty \rho_{2i}(x, y, t) dx dy \quad (i = 1, 2).$$

If during the process the maximum distance between the centers of mass  $\Delta = \max_t |y_{c1}(t) - y_{c2}(t)|$  exceeded the initial diameter  $2R$  of the cloud, then the cloud was considered to have separated.

The calculations showed that when the relative volume fraction of the particle changed over two orders of magnitude ( $0.1 \leq \alpha_{21}^0/\alpha_{22}^0 \leq 10$ ), the value of  $\Delta$  for a fixed volume composition of all the dispersed phase changes weakly (by no more than 10%). Therefore in all

calculations of  $\Delta$ , the volume fractions of particles of different dimensions were chosen to be the same:  $\alpha_{21}^0 = \alpha_{22}^0 = \alpha_2^0/2$ . Outside this region, the changes in the ratio  $\alpha_{21}^0/\alpha_{22}^0$  of the density of the particles of one type in the cloud are much larger than the density of particles of the other type. Therefore the characteristics of the falling and sedimentation of the cloud can be estimated from published results for the corresponding monodispersed cloud [2, 9].

Considering this discussion, the position of the boundary in space of the parameters (1.9) depends on the variables  $\delta_1$ ,  $\delta_2$ ,  $\alpha_2^0$ ,  $Re^0$ , and  $H$ . The first four determine the physical characteristics of the dispersed phase and the suspending medium, and the last, the initial position of the cloud above the underlying surface. This position can have a large effect on the behavior of the boundary. Below, we investigate the position of the boundary curve as a function of these five parameters.

The effect of  $\delta_1$  and  $\delta_2$  is illustrated in Fig. 1. For fixed values of  $\alpha_2^0 = 10^{-3}$  and  $Re^0 = 6.5 \cdot 10^6$ , graphs are constructed which divide the two sedimentation regimes of the cloud (curves 1-3 for  $H = 5, 10.3,$  and  $15.3$ ) in the coordinates  $\delta_1/\delta_2$  and  $\log \delta^0$ , where  $\delta^0 = \delta_1 + \delta_2$ . To the left of the boundary lies the region of parameters for which the cloud separates ( $\Delta > 2R$ ); to the right, the region of combined sedimentation ( $\Delta < 2R$ ).

The behavior of curves 2 and 3, which correspond to rather large initial heights, is explained as follows. It is clear that the bidispersed cloud, which consists of particles with  $\delta_1/\delta_2 \approx 1$  will not separate (in the limit  $\delta_1/\delta_2 \rightarrow 1$  it transforms into a monodispersed cloud). Conversely, a cloud consisting of particles whose diameters are very different ( $\delta_1/\delta_2 \rightarrow 0$ ) surely separate. Consequently, for each fixed value of  $\delta^0$ , there is a ratio of diameters  $\delta_1/\delta_2$  which corresponds to a separation boundary  $\Delta = 2R$ . If the ratio  $\delta_1/\delta_2$  and decrease in the dimensions of particles of both types are fixed, then the hydrodynamic interactions between the aerosol particles will increase [2, 9], which means that the value of  $\Delta$  will decrease, and there will be a transition to the combined sedimentation regime.

The lower the initial height of the cloud, the smaller the allowable value of  $\Delta$  over the falling time; therefore curve 2 lies above curve 3. All three boundary curves, which correspond to different initial heights, asymptotically approach the ordinate in the range of small particle dimensions ( $\delta^0 \approx 10^{-4}$ ), due to the strong hydrodynamic interaction of the solid particles with the suspending gas. As a result, the separation of the cloud can occur only for large dimensional differences in the particle dimensions ( $\delta_1/\delta_2 \rightarrow 0$ ) and in their characteristic sedimentation velocities. In the range of rather large particle diameters ( $\delta^0 \approx 5 \cdot 10^{-4}$ ), the aerosol formation settles much faster as a whole and the behavior of the boundary curves depends more strongly on the initial height of the cloud. If  $H$  is small (curve 1), the particles of both types cannot separate, even for large diameter differences, over the time for them to fall a distance  $\Delta > 2R$ , which is required to cause separation. Therefore, for small  $H$ , the boundary curves shift to the ordinate.

From Fig. 1 it can be seen that the difference in the position of the boundary curves 2 and 3 is much less than between 1 and 2, and the difference appears for large values of  $\delta^0$ . Therefore, one can expect that for large  $H$ 's, there exists an envelope of boundary curves, constructed for various heights (although no calculations were done with  $H > 15.3$ ).

The effect of the parameters  $\alpha_2^0$  and  $Re^0$  on the position of the boundary is shown in Fig. 2 in the same coordinates as in Fig. 1. For a fixed height  $H = 5$ , boundary curves of clouds are constructed with  $\alpha_2^0 = 2 \cdot 10^{-3}, 10^{-3},$  and  $10^{-4}$ , and for  $Re^0 = 6.5 \cdot 10^6$  (curves 1-3, respectively); and for  $Re^0 = 10^6$  and  $2.6 \cdot 10^7$  with  $\alpha_2^0 = 10^{-3}$  (curves 4 and 5). Because the increase in the volume content of the dispersed phase leads to an increase in interaction between particles through the carrier gas [2, 9], the region which corresponds to combined sedimentation expands, and the boundary curves approach the ordinate. The effect of the parameter  $Re^0$  is illustrated by curves 2, 4, and 5. The growth in  $Re^0$  can be interpreted as an increase in the cloud radius, which for fixed  $\delta_1$  leads to a growth in the particle diameters  $d_i$  and, as a result, a decrease in their concentration  $n_i = 6\alpha_{2i}/(\pi d_i^3)$ , that is, to a weakening of the hydrodynamic interaction of the particles with each other [2, 9]. Therefore, as  $Re^0$  is increased, the separation boundary is shifted to the right. If the growth in  $Re^0$  is interpreted as a lowering of the molecular kinematic viscosity of the gas  $\eta/\rho_{10}$ , then the behavior of the boundary curves is explained by the weakening in the interaction between the particles as a result of the decreased thickness of the boundary layer around the particles [10].

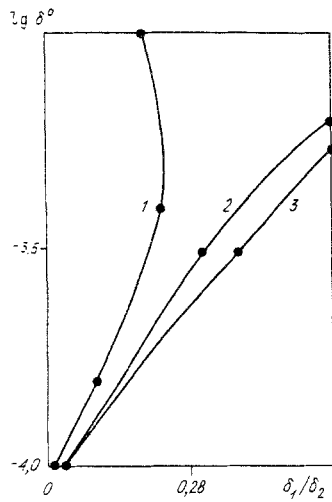


Fig. 1

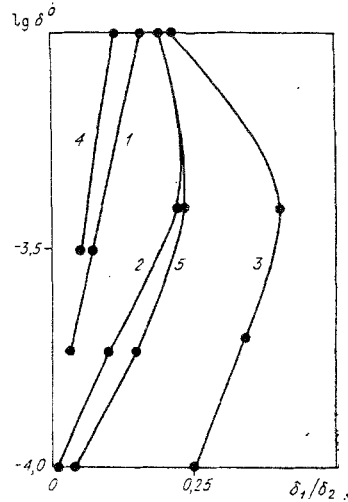


Fig. 2

3. The regime of combined sedimentation occurs when the hydrodynamic interaction between the particles of different diameters is rather strong.

A characteristic distribution pattern of particle density and the velocity field of the gas are shown in Fig. 3 for two sequential times:  $t = 2.10$  and  $5.24$  for Figs. 3a and 3b ( $\delta_1 = 6.67 \cdot 10^{-5}$ ,  $\delta_2 = 1.33 \cdot 10^{-4}$ ,  $\alpha_{21}^0 = 7 \cdot 10^{-4}$ , and  $\alpha_{22}^0 = 3 \cdot 10^{-4}$ ). Hereafter for this discussion  $Re^0 = 6.5 \cdot 10^6$  and  $H = 5$ . To the right of the surface of symmetry are shown the curves of equal density of fine particles [on isocurves 1,  $\rho_{21}(1) = 0.1$ , with a step  $\Delta\rho = 0.1$ ] and the velocity field of the gas (the velocity scale is shown in the upper right corner); to the left are the density isocurves of the larger particles [ $\rho_{22}(1) = 0.05$  and  $\Delta\rho = 0.05$ ]. The parameters of the dispersed phase in the monodispersed cloud regime are chosen so that if the particle of each type settles separately in the monodispersed cloud, then the fine particles would be carried away, and the larger ones would settle in the filtration regime [2, 9]. For combined sedimentation, when some amount of large particles are added to the fine ones ( $\alpha_{21}^0/\alpha_{22}^0 = 0.43$ ) in the bidispersed cloud, the large ones are entrained in the vortical motion of the gas which arises from the fine ones (see the velocity field of the gas in Fig. 3b), and the entrainment regime is also realized for the large ones: the first circular concentric isocurves of density of the second type (Fig. 3a) are distorted, and the cloud takes on a bowl shape (Fig. 3b).

4. For a quantitative characteristic of the degree of hydrodynamic interaction of the dispersed phase with the suspending gas and the particle dispersion along the underlying surface, it is convenient to introduce a dispersion coefficient for particles of the dispersed phase as in [2, 9]:

$$m = 1 - \int_0^1 \rho_2^s(x, \infty) dx \Big/ \int_0^1 dx \int_0^\infty \rho_2(x, y, 0) dy, \quad (4.1)$$

$$\rho_2^s = \rho_{21}^s + \rho_{22}^s, \quad \rho_2(x, y, 0) = \rho_{21}(x, y, 0) + \rho_{22}(x, y, 0).$$

Here  $\rho_2^s(x, \infty)$  is the final distribution of particles of both types, which have fallen onto the underlying surface, and  $\rho_2(x, y, 0)$  is the initial distribution of the dispersed phase in the region. Physically, the dispersion coefficient is equal to the mass fraction of the dispersed phase which has fallen onto the underlying surface outside the geometric shadow of the initial cloud. The more intense the hydrodynamic interaction of the finely dispersed particles with the suspending gas, the more powerful the vortical motion of the gas motion when the cloud settles out. It can carry the particles laterally and increase the particle dispersion coefficient.

In analogy to (4.1), one can introduce a dispersion coefficient of each type of particle when it settles out in the composition of the bidispersed cloud:

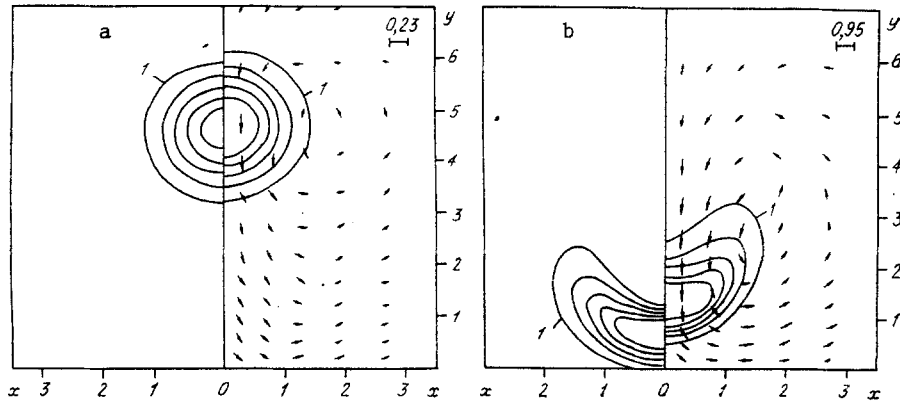


Fig. 3

$$m_i = 1 - \int_0^1 \rho_{2i}^s dx \Big/ \int_0^1 dx \int_0^\infty \rho_{2i}(0) dy \quad (i = 1, 2). \quad (4.2)$$

On the other hand, the dispersion coefficient  $m_i^0$  for each type particle which settles out of a monodispersed cloud (in the absence of the second type of particle) can be determined from the sedimentation solution for a monodispersed cloud. The difference in the coefficients  $m_i$  and  $m_i^0$  quantitatively characterizes the difference between the sedimentation of particles of each type in the composition of the dispersed and monodispersed clouds.

These differences are illustrated in Fig. 4, where curves 1 and 2 represent the final distributions of particles of each type, which have fallen onto the underlying surface (all cloud parameters are the same as in Fig. 3). For comparison, the final distributions of the particle densities of each type are presented for the monodispersed regime (curve 1' is for the fine particles and 2' is for the large ones). The distribution  $\rho_{22}^s$  (curve 2) is greatly stretched out along the sedimentation surface compared to the sedimentation of the monodispersed cloud (curve 2'), and the dispersion coefficient in the bidispersed cloud rises correspondingly - from  $m_2^0 = 0.33$  in the monodispersed cloud to  $m_2 = 0.50$  in the bidispersed cloud; that is, by more than 50%. We note that according to [2], the boundary between the filtration and entrainment regimes for particles of the second type at a fixed height  $H = 5$  corresponds to a dispersion coefficient  $m_x = 0.40$ . The distribution  $\rho_{21}^s$  changes much less, as compared with a single sedimentation (see curves 1 and 1'), than for larger particles; as a result, the change in the dispersion coefficient is small:  $m_1^0 = 0.71$  and  $m_1 = 0.62$ . From this example it can be seen that an intense interaction between the two types of particles is observed in the combined sedimentation regime of the bidispersed cloud, as opposed to the separation regime.

It follows from (4.1) and (4.2) that the particle dispersion coefficient in the bidispersed cloud is the sum of "partial" dispersion coefficients  $m_1$  and  $m_2$ , which multiply the fraction of the particles of each type in the dispersed cloud, that is

$$m = (\alpha_{21}^0/\alpha_2^0)m_1 + (\alpha_{22}^0/\alpha_2^0)m_2. \quad (4.3)$$

If each of the two dispersed phases settled out independently, the values  $m_i$  in (4.3) would be equal to the corresponding values  $m_i^0$  obtained by solving the sedimentation problem for a monodispersed cloud. Therefore the difference between  $m$  and the coefficient

$$m^0 = (\alpha_{21}^0/\alpha_2^0)m_1^0 + (\alpha_{22}^0/\alpha_2^0)m_2^0, \quad (4.4)$$

which is constructed for the monodispersed values  $m_i^0$ , characterizes the interaction between the particles of both types: the larger the difference  $m - m^0$ , the stronger the interaction.

Figure 5 shows the behavior of the dispersion coefficients  $m$  and  $m^0$  and the difference (curves 1-3) for a fixed fraction of the dispersed phase  $\alpha_2^0 = 10^{-3}$  for particles with diameters  $\delta_1 = 1.33 \cdot 10^{-5}$  and  $\delta_2 = 6.67 \cdot 10^{-5}$ . The curves marked with primes correspond to  $\delta_1 = 6.67 \cdot 10^{-5}$  and  $\delta_2 = 1.33 \cdot 10^{-4}$ . The abscissa is  $\alpha_{21}^0/\alpha_2^0$  - the ratio of the volume composition of fine particles  $\alpha_{21}^0$  to the sum of the volume composition of the dispersed phase.

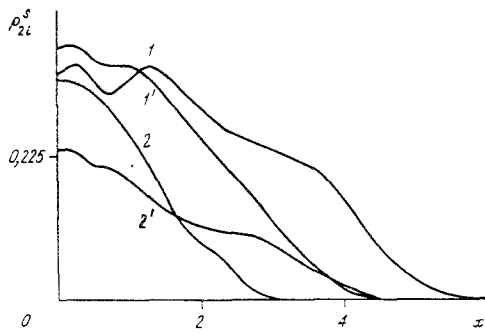


Fig. 4

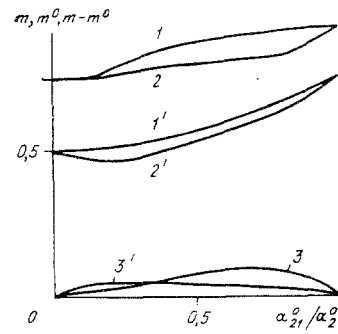


Fig. 5

The change in  $\alpha_{21}^0/\alpha_2^0$  denotes that a fixed mass of the solid or liquid material

$$M_0 = \int_0^\infty \int_0^\infty [(\alpha_{21}^0 + \alpha_{22}^0)/\varepsilon \exp(-(x^2 + (y-H)^2))] dx dy$$

disperses in different proportions for the particles of two diameters and scatters in a region of the fixed radius  $R$ . If  $\alpha_{21}^0/\alpha_2^0$  is small, the cloud consists basically of large particles of diameter  $\delta_2$ ; if  $\alpha_{21}^0/\alpha_2^0 \rightarrow 1$ , then the composition of the bidispersed aerosol approximates the composition of the monodispersed cloud of fine particles with diameter  $\delta_1$ .

From Fig. 5 it can be seen that when  $\alpha_{21}^0/\alpha_2^0$  is close to unity or zero, the difference  $m - m^0$  tends to zero as expected. The largest difference between the coefficients  $m$  and  $m^0$  is observed for some intermediate value of  $\alpha_{21}^0/\alpha_2^0$ . For  $\delta_1 = 6.67 \cdot 10^{-5}$  and  $\delta_2 = 1.33 \cdot 10^{-4}$ , the maximum difference  $m - m^0$  (curve 3') is substantially less, almost by a factor of two, than for  $\delta_1 = 1.33 \cdot 10^{-5}$  and  $\delta_2 = 6.67 \cdot 10^{-5}$  (curve 3). This is explained by the fact that decreasing the diameter of the particles strengthens their interaction with the suspending gas and therefore increases the difference  $m - m^0$ .

We note that, although the values  $m$  and  $m^0$  differ, the coefficient  $m^0$  gives a qualitatively correct description of the behavior of the dispersion coefficient of the bidispersed cloud and can be used as a lower bound for  $m$ . Thus, knowing the dispersion coefficients of monodispersed clouds and having calculated  $m^0$  from (4.4), it is possible to predict the behavior of the bidispersed cloud. In this parameter range, such an estimate gives an error of no more than 15%.

The numerical study of sedimentation of a cloud of a bidispersed aerosol leads to the following conclusions.

There are two qualitatively different sedimentation regimes of a bidispersed cloud: separation and combined sedimentation of both types. In the disintegration regime, the bidispersed cloud separates into two independently sedimentation aggregates, whose behavior is analogous to the behavior of the corresponding monodispersed clouds. Therefore, for studying this regime it is unnecessary to do additional investigations. In the space of the defining parameters  $\alpha_2^0$ ,  $\delta_1$ ,  $Re^0$ , and  $H$  for the selected region of application, we studied the behavior of the boundary between the separation regime and the combined sedimentation regime.

In the combined sedimentation regime, there is a strong hydrodynamic interaction between the particles with various dimensions, and therefore a bidispersed cloud settles as a single formation. Here a mutual effect of the particles of different diameters on each other is observed. On one hand, the larger particles are entrained in the vortical motion of the gas induced by the smaller particles, which leads to an increased dispersion coefficient of the larger particles, as compared to the sedimentation of the corresponding monodispersed cloud. On the other hand, the large particles "slow" the gas vortex, and therefore the dispersion coefficient is less for the smaller particles in the bidispersed cloud than for the corresponding monodispersed cloud.

Thus, the behavior of the bidispersed cloud in the combined sedimentation regime is significantly different from the behavior of the monodispersed cloud, which consists of particles of some single dimension. However, by knowing the dispersion coefficient for particles of each type onto the underlying surface from the sedimentation in the composition of the

monodispersed cloud, from Eq. (4.4) it is possible to get a lower estimate for the dispersion coefficient of the bidispersed cloud and to predict its behavior.

#### LITERATURE CITED

1. N. A. Fuks, *Mechanics of Aerosols* [in Russian], Izd. Akad. Nauk SSSR, Moscow (1959).
2. G. M. Makhviladze and O. I. Melikhov, "The motion of an aggregate of particles under the influence of gravity and its sedimentation onto a horizontal surface," *Izv. Akad. Nauk SSSR, Mekh. Zhidk. Gaza*, No. 6 (1982).
3. J. M. Burgers, "Influence of the concentration of a suspension upon the sedimentation velocity," *Prok. Kon. Nederl. Akad. Wet.*, 44, No. 9 (1941).
4. V. V. Struminskii, O. B. Gus'kov, and Yu. N. Kul'bitskii, "Hydrodynamics of dispersed and gas-liquid flows," *Dokl. Akad. Nauk SSSR*, 278, No. 1 (1984).
5. A. L. Drofman, "Numerical solution of two-phase flow in a viscous entraining medium," *Izv. Akad. Nauk SSSR, Mekh. Zhidk. Gaza*, No. 3 (1981).
6. G. M. Makhviladze and O. I. Melikhov, "Sedimentation of a cloud of a gas suspension onto a horizontal surface," *Prikl. Mekh. Tekh. Fiz.*, No. 2 (1987).
7. R. I. Nigmatulin, *Dynamics of Monophase Media* [in Russian], Part I, Nauka, Moscow (1987).
8. G. M. Makhviladze and O. I. Melikhov, "Large-scale vortical motion in the falling and sedimentation of an aggregate of monodispersed particles, *ChMMS*, 13, No. 4 (1982).
9. G. M. Makhviladze and O. I. Melikhov, "Numerical investigation of the falling of an aggregate of monodispersed particles onto a plane horizontal surface," Preprint No. 191, Institute of Problems in Mechanics, Russian Academy of Sciences, Moscow (1981).
10. L. G. Loitsyanskii, *Mechanics of Liquid and Gas* [in Russian], Nauka, Moscow (1987).